Studies of molybdenum compounds. 5. Diethyl(2,2'-bipyridyl)dioxomolybdenum(VI) and other higher dialkyl derivatives of dioxomolybdenum(VI)

G. N. Schrauzer, E. O. Schlemper, Liu Nan. Hui, K. Rubin, Ximu. Zhang, Xiping. Long, and Chong Shik. Chin

Organometallics, **1986**, 5 (12), 2452-2456• DOI: 10.1021/om00143a008 • Publication Date (Web): 01 May 2002

Studies of Molybdenum Compounds. 5. Diethyl(2,2′-bipyridyl)dioxomolybdenum(VI) and Other Higher Dialkyl Derivatives of Dioxomolybdenum(VI)

G. N. Schrauzer,* E. O. Schlemper,* Nan Hui Liu,[1] Qiguang Wang,[1] K. Rubin, Xumu Zhang, Xiping Long, and Chong Shik Chin[2]

Department of Chemistry, University of California, San Diego, Revelle College, La Jolla, California 92093

Received November 5, 1985

The synthesis of diethyl(2,2′-bipyridyl)dioxomolybdenum(VI) and of other higher dialkyl derivatives of complexes of composition $R_2Mo(O)_2(bpy)$ (R = C_2H_5, *n*- and *i*-C_3H_7, *n*- and *i*-C_4H_9, c-C_5H_9, c-C_6H_{11}; bpy = 2,2′-bipyridyl) from $Br_2Mo(O)_2(bpy)$ and organomagnesium halides by a modification of a previously reported method is described. The complex $(C_2H_5)_2Mo(O)_2(bpy)$ crystallizes from CH_2Cl_2 in the trigonal space group $P3_121$ with $a = b = 8.409$ (3) Å and $c = 40.69$ (1) Å, with $Z = 6$, with $^1/_2$ mol of CH_2Cl_2/mol of complex. Average bond distances in the planar $Mo(O)_2(bpy)$ moiety are similar to those observed in other complexes of this type (Mo=O = 1.702 (1) and Mo—N = 2.325 (12) Å). The in-plane O–Mo–O and N–Mo–N bond angles are also normal. Although the complex is much less stable thermally than the corresponding methyl derivative, the average Mo–C bond distances of 2.20 (2) Å are virtually the same as in the dimethyl species. However, the C–Mo–C bond angle of 151.9° is 2.9° wider than in the dimethyl and 3.8° narrower than in the dineopentyl derivative. These differences are attributed to interactions of the terminal ethyl hydrogen atoms with the oxygen atoms of the $Mo(O)_2$ moiety. Thermolysis, photolysis, and acid hydrolysis of the Mo–C bonds produces mixtures of unrearranged olefins and alkanes as principal products. The cleavage of one Mo–C bond occurs mainly by way of β-elimination which induces the reductive cleavage of the other. Traces of higher hydrocarbons arising from Mo–C bond homolysis reactions are formed on thermolysis and photolysis of the solid complexes.

Introduction

The exploration of the organometallic chemistry of molybdenum(VI) thus far produced only a relatively small number of compounds carrying organic substituents with hydrogen atoms in β-position relative to the metal. Although we have previously[3] reported the synthesis of higher *n*-alkyl derivatives of complexes of the type R–$Mo(O)_2(bpy)Br$, as well as of higher monoalkyl anions R–MoO_3^{3-}, molybdenum complexes carrying two or more β-hydrogen carrying alkyl residues thus far could be obtained. Thus, while the reaction of $Br_2Mo(O)_2(bpy)$ (1, bpy = 2,2′-bipyridyl) with organomagnesium halides afforded the remarkably stable complexes $R_2Mo(O)_2(bpy)$ with R = CH_3 (2),[4] neopentyl (3),[5] or benzyl (4),[6] none of the corresponding higher di-*n*-alkyl derivatives could be obtained. Similarly, the studies of Schrock[7] and Osborn[8] on group VI (6[11]) organometallic compounds were essentially restricted to the methyl and neopentyl derivatives. By a modification of the initial synthesis technique we have now succeeded in preparing a number of higher primary, secondary dialkyl and dicycloalkyl derivatives of compounds of composition $R_2Mo(O)_2(bpy)$ and thus were able to compare their properties and reactions with those of the previously known compounds. The structure of the prototype complex with R = C_2H_5 (5) was also determined.

Experimental Section

Reagents and Chemicals. All commercially available reagents and chemicals of "analytical" or "reagent grade" purity were used without further purification. Alkyl bromides for synthesis of the organomagnesium bromides were fractionally distilled before use. Tetrahydrofuran (Mallinckrodt) was dried over potassium and distilled immediately before use. $Mo(O)_2(Br)_2(bpy)$ (1) was prepared according to Hull and Stiddard.[9]

Synthesis of $Mo(O)_2(C_2H_5)_2(bpy)$ (5). To a stirred suspension of 2 g (4.5 mmol) of I in 50 cm^3 of dry tetrahydrofuran (THF) was added 18 mmol of ethylmagnesium bromide in 50 cm^3 of THF dropwise under argon at 0 °C over a period of 15 min. (A 1 M solution of ethylmagnesium bromide was prepared from 16 g of freshly distilled ethyl bromide in 50 cm^3 of THF and 12 g of Mg suspended in 200 cm^3 of THF at 0 °C under argon; aliquots of this solution were diluted with dry THF before use, as indicated above.) The reaction solution was kept at 0 °C for another 15 min and was subsequently evaporated in vacuo at room temperature. After the addition of 250 cm^3 of CH_2Cl_2, the solution was shaken repeatedly with portions of 100 cm^3 of water in a separatory funnel; the water extracts were removed and discarded; the yellow CH_2Cl_2 solution was dried with anhydrous $MgSO_4$ and concentrated to 25 mL through vacuum evaporation at room temperature. From this solution, pale yellow crystals of $(C_2H_5)Mo(O)_2(bpy)$ with some CH_2Cl_2 of crystallization separated after the addition of *n*-hexane. These were collected by vacuum filtration, washed with hexane, and dried: yield 1.1 g (71% based on 1); mp 138 °C dec. Anal. Calcd for $C_{14}H_{18}N_2O_2Mo$: C, 49.13; H, 530; Mo, 28.03; N, 8.18; O, 9.35; M_r, 342.24. Found, C, 48.90; H, 5.04; Mo, 27.91; N, 8.14; O, 10.01, M_r, 425 (cryoscopic in benzene). ^1H NMR [in $CDCl_3$, ppm (intensities)]: 7.3–9.8 (8),

(1) Present address: Lanzhou University, Lanzhou, Gansu, China.
(2) On leave of absence from Sogang University, Seoul, Korea.
(3) (a) Hughes, L. A.; Liu, Nan Hui; Schrauzer, G. N. *Organometallics* **1983**, *2*, 486. (b) Schrauzer, G. N.; Hughes, L. A.; Strampach, N. *Z. Naturforsch. B: Anorg. Chem., Org. Chem.* **1982**, *37B*, 380.
(4) Schrauzer, G. N.; Hughes, L. A.; Strampach, N.; Robinson, P. R.; Schlemper, E. O. *Organometallics* **1982**, *1*, 44.
(5) Schrauzer, G. N.; Hughes, L. A.; Strampach, N.; Ross, F.; Ross, D.; Schlemper, E. O. *Organometallics* **1983**, *2*, 481.
(6) Schrauzer, G. N.; Hughes, L. A.; Schlemper, E. O.; Ross, F.; Ross, D. *Organometallics* **1983**, *2*, 1163.
(7) Clark, D. N.; Schrock, R. R. *J. Am. Chem. Soc.* **1978**, *100*, 6774.
(8) Kress, J. M. R.; Russell, M. J. M.; Wesolek, M. G.; Osborn, J. A. *J. Chem. Soc., Chem. Commun.* **1980**, 431.
(9) Hull, C. G.; Stiddard, M. H. B. *J. Chem. Soc.* **1966**, 1633.
(10) *International Tables for Crystallography*; Kynoch Press: Birmingham, England, 1974; Vol. IV.
(11) In this paper the periodic group notation is in accord with recent actions by IUPAC and ACS nomenclature committees. A and B notation is eliminated because of wide confusion. Groups IA and IIA become groups 1 and 2. The d-transition elements comprise groups 3 through 12, and the p-block elements comprise groups 13 through 18. (Note that the former Roman number designation is preserved in the last digit of the new numbering: e.g., III 3 and 13.)

0276-7333/86/2305-2452$01.50/0

Table I. Crystallographic, Data Collection, and Refinement Parameters

formula	$MoO_2N_2C_{14}H_{18}\cdot{}^1/_2(CH_2Cl_2)$	λ, Å (Mo Kα)	0.7107
$a = b$, Å	8.409 (3)	μ, cm^{-1}	9.4
c, Å	40.69 (1)	ψ scan transmissn correctn range	0.95–1.00
cryst system	trigonal		
space group	$P3_121$	scan speed variable to maintain 3% counting statistics to max time of 90 s	
V, $Å^3$	2491 (1)		
ρ_{calcd}, g cm^{-3}	1.538 (2)	scan mode	θ–2θ
Z	6		
M_r	384.7		
total no. of observn	3874	scan width, deg	0.70 + 0.35 tanθ
no. of independent refl	1821	data limits, 2θ deg	2–45
no. of independent refl with $F_o > 2\sigma(F_o)$ used in refinement	1601	monochromation	graphite crystal
no. of variables	186		
$R(F_o)$	0.051	largest shift/error	0.01
$wR(F_o)$	0.071	max ρ (e/$Å^3$) on final diff Fourier	0.9

bpy protons; 1.34 (10), C_2H_5 protons. For UV–vis (λ_{max}) and IR spectral data, see Table VI.

Structural Analysis. Crystals suitable for single X-ray diffraction studies were obtained from dichloromethane. These contain 0.5 mol of CH_2Cl_2/molecule of complex which is lost slowly during data collection. About 25% decomposition in 48 h was observed for three standard reflections which were measured every 100 reflections so that two crystals were used with data overlap to allow appropriate scaling. Epoxy coating did not significantly slow the decay. The data from both crystals were corrected for decomposition and for absorption (empirical ψ scan method) before merging. Merging with "hand" reversal on one date set gave slightly poorer $R_{int.}$ (0.042 vs. 0.048). The data were measured on an Enraf-Nonius CAD4 automated diffractometer. Table I gives the crystallographic data, data collection parameters, and refinement details. The unit cell parameters were determined by least-squares fit of the setting angles of 25 reflections which were automatically centered on the diffractometer. The three intensity standards were measured after every 7200 s of X-ray exposure and were used to make the decomposition correction. Orientation was checked after every 200 reflections with three standards, and all 25 reflections were recentered to obtain a new matrix when needed.

The structure was solved by conventional Patterson and difference Fourier techniques. Least-squares refinement minimized $\sum w(F_o - F_c)^2$, where $w = 4F_o^2/\sigma_{counting}^2 + (0.05F_o^2)^2)$. Hydrogen atoms were either located from difference Fourier syntheses or placed in chemically reasonable positions and were not refined. All other atoms were refined with anisotropic thermal parameters. The terminal methyl carbon atoms show rather high thermal motion corresponding to hindered rotation resulting in apparent shortening of the C–C bonds. Atomic scattering factors were taken from ref 1 and included anomalous scattering factors. Refinement of the opposite hand of the molecular in $P3_21$ gave $R = 0.052$ and $wR = 0.072$.

Final positional parameters and isotropic equivalent thermal parameters are included in Table II for non-hydrogen atoms. Selected interatomic distances and angles are given in Tables III and IV, respectively. F_o and F_c values and anisotropic thermal parameters are available as supplementary material.

Synthesis of Related Complexes. Complexes **6**–**11** were obtained with yields from 60–80% in analogy to the method given above for the diethyl derivative. See Table V for analytical data.

Physical Properties. Table VI summarizes the observed λ_{max} in the UV–vis spectra and the IR $\nu_{Mo=O}$ stretching frequencies.

Chemical Properties. Thermolysis. Experiments were conducted with 4 mg (0.9 μmol) of **5** in serum-capped Pyrex test tubes of 10 cm^3 capacity that were either filled with argon, hydrogen, or oxygen, all at 1 atm. One series of experiments was also performed in 0.5 mL of silicone bath oil as a solvent (0.5 cm^3) under argon. Hydrocarbons were identified by comparison of the retention times and coinjection of authentic samples of hydrocarbons as well as by mass spectrography, employing a Hewlett-Packard Model 700 gas chromatograph fitted with an 8 ft × $^1/_8$ in. column packed with phenyl isocyanate on Porasil C operating at 50 °C with and FID detector and a LKB 9000 mass spectrograph. Hydrogen was measured by GLPC using a column of 6 ft × $^1/_8$ in. filled with molecular sieves (5 Å) operating at 27 °C and employing TC detection. Results of thermolysis experiments are summarized in Table VII.

Photolysis. Samples of 4 mg of **5** in argon-filled, serum-capped Pyrex test tubes were exposed to the light emitted from a water-cooled 360-W Hg-arc Hanovia UV lamp at a distance of 10 cm. For the photolysis experiments in methanolic solution or aqueous suspension, 1 cm^3 of CH_3OH or H_2O was injected immediately prior to irradiation. Analyses for gaseous products were performed as outlined above; results are summarized in Table VIII.

Table II. Positional Parameters and Their Estimated Standard Deviations[a]

atom	x	y	z	B, $Å^2$
Mo	−0.16304 (9)	−0.2850 (1)	0.08820 (2)	3.71 (2)
Cl	0.1688 (6)	0.3362 (6)	0.0181 (1)	13.1 (2)
O1	−0.0447 (8)	−0.230 (1)	0.0524 (2)	5.2 (2)
O2	−0.0505 (8)	−0.3360 (8)	0.1177 (2)	5.2 (2)
N2	−0.3968 (9)	−0.3433 (9)	0.1257 (2)	3.6 (2)
N1	−0.3890 (8)	−0.2439 (8)	0.0641 (2)	3.1 (2)
C1	−0.369 (1)	−0.569 (1)	0.0744 (3)	6.2 (3)
C2	−0.087 (1)	−0.088 (1)	0.1043 (3)	6.6 (3)
C3	−0.369 (1)	−0.178 (1)	0.0334 (2)	4.2 (2)
C4	−0.500 (1)	−0.152 (1)	0.0175 (3)	4.9 (3)
C5	−0.657 (1)	−0.191 (1)	0.0356 (3)	4.8 (3)
C6	−0.677 (1)	−0.257 (1)	0.0675 (3)	4.8 (3)
C7	−0.545 (1)	−0.286 (1)	0.0812 (3)	3.9 (2)
C8	−0.550 (1)	−0.346 (1)	0.1149 (2)	3.4 (2)
C9	−0.698 (1)	−0.392 (1)	0.1360 (2)	4.3 (3)
C10	−0.687 (1)	−0.444 (1)	0.1684 (3)	5.6 (3)
C11	−0.529 (1)	−0.439 (1)	0.1780 (3)	5.6 (3)
C12	−0.392 (1)	−0.388 (1)	0.1564 (2)	4.7 (3)
C13	−0.292 (2)	−0.691 (2)	0.0702 (3)	7.3 (4)
C14	0.113 (2)	0.103 (2)	0.1085 (5)	15.2 (7)
C15	0.148 (3)	0.148	0.000	11.4 (7)

[a] Anisotropically refined atoms are given in the form of the isotropic equivalent displacement parameter defined as $(^4/_3)[a^2\beta(1,1) + b^2\beta(2,2) + c^2\beta(3,3) + ab(\cos\gamma)\beta(1,2) + ac(\cos\beta)\beta(1,3) + bc(\cos\alpha)\beta(2,3)]$.

Table III. Bond Distances (Å)[a]

atom 1	atom 2	dist	atom 1	atom 2	dist
Mo	O1	1.695 (6)	C1	C13	1.39 (1)
Mo	O2	1.709 (5)	C2	C14	1.47 (2)
Mo	N2	2.338 (6)	C3	C4	1.38 (2)
Mo	N1	2.313 (6)	C4	C5	1.40 (1)
Mo	C1	2.21 (2)	C5	C6	1.39 (1)
Mo	C2	2.193 (8)	C6	C7	1.37 (2)
Cl	C15	1.674 (7)	C7	C8	1.46 (1)
N2	C8	1.347 (9)	C8	C9	1.41 (1)
N2	C12	1.311 (9)	C9	C10	1.41 (2)
N1	C3	1.342 (9)	C10	C11	1.36 (1)
N1	C7	1.364 (9)	C11	C12	1.34 (1)

[a] Numbers in parentheses are estimated standard deviations in the least significant digits.

Table IV. Bond Angles (deg)

atom 1	atom 2	atom 3	angle	atom 1	atom 2	atom 3	angle
O1	Mo	O2	110.4 (3)	Mo	N1	C3	121.0 (4)
O1	Mo	N2	159.4 (2)	Mo	N1	C7	119.9 (5)
O1	Mo	N1	90.5 (2)	C3	N1	C7	119.1 (6)
O1	Mo	C1	96.4 (3)	Mo	C1	C13	112.7 (7)
O1	Mo	C2	99.0 (4)	Mo	C2	C14	109.9 (7)
O2	Mo	N2	90.2 (2)	N1	C3	C4	123.8 (7)
O2	Mo	N1	159.2 (2)	C3	C4	C5	116.7 (7)
O2	Mo	C1	98.0 (3)	C4	C5	C6	119.4 (6)
O2	Mo	C2	98.5 (3)	C5	C6	C7	120.6 (7)
N2	Mo	N1	69.0 (2)	N1	C7	C6	120.3 (8)
N2	Mo	C1	79.5 (3)	N1	C7	C8	115.3 (6)
N2	Mo	C2	77.8 (3)	C6	C7	C8	124.1 (7)
N1	Mo	C1	78.2 (3)	N2	C8	C7	116.1 (6)
N1	Mo	C2	78.2 (3)	N2	C8	C9	121.2 (7)
C1	Mo	C2	151.9 (3)	C7	C8	C9	122.7 (6)
Mo	N2	C8	119.1 (5)	C8	C9	C10	118.1 (7)
Mo	N2	C12	122.8 (5)	C9	C10	C11	118.3 (8)
C8	N2	C12	117.9 (6)	C10	C11	C12	119.3 (8)
				N2	C12	C11	125.3 (8)

[a] Numbers in parentheses are estimated standard deviations in the least significant digits.

Table V. Analytical Data for Complexes 6–11

no.	mp, dec	compositn	analysis: calcd C	calcd H	calcd Mo	found C	found H	found Mo
6	151	$C_{16}H_{20}MoN_2O$	52.18	5.47	26.05	51.74	5.33	26.02
7	120	$C_{18}H_{22}MoN_2O_2$	54.83	5.62	24.33	54.44	5.60	24.52
8	156	$C_{18}H_{22}MoN_2O_2$	54.83	5.62	24.33	54.64	5.62	24.05
9	141	$C_{18}H_{22}MoN_2O_2$	54.83	5.62	24.33	54.74	5.68	24.82
10	117	$C_{20}H_{24}MoN_2O_2$	57.14	5.75	22.82	57.44	5.92	23.00
11	105	$C_{22}H_{26}MoN_2O_2$	59.19	5.87	21.49	59.05	5.78	21.22

[a] Decomposition.

Table VI. Summary of Physical Properties of Complexes 5–11

no.	R	UV–vis λ_{max}, nm (ϵ)	IR $\nu_{Mo=O}$, cm^{-1}
5	C_2H_5	361 (2200), 300 (18 500), 288 (s), 247 (25 400)	934, 905
6	n-C_3H_7	358 (2100), 300 (19 000), 287 (s), 249 (25 500)	926, 889
7	i-C_3H_7	362 (2000), 301 (18 600), 285 (s), 245 (25 000)	914, 882
8	n-C_4H_9	356 (2100), 301 (19 000), 290 (s), 248 (25 400)	933, 901
9	i-C_4H_9	386 (1950), 306 (18 7000), 298 (s), 246 (25 500)	932, 898
10	c-C_5H_9	380 (2050), 301 (18 900), 288 (s), 256 (25 400)	914, 882
11	c-C_6H_{11}	408 (1850), 300 (18 600), 287 (s), 258 (25 500)	919, 890

Table VII. Gas-Phase Products of Thermolysis of 5 under Various Conditions

products	% yields[a] under thermolysis conditns: Ar	H_2	O_2	silicone oil[b]
H_2	1.47		0.54	0.16
CH_4	0.33	0.36	0.12	0.13
C_2H_6	53.9	52.9	49.8	55.4
C_2H_4	29.7	29.3	34.2	34.7
C_3H_8	0.022	0.022	0.033	0.022
C_4H_{10}	0.31	0.32	0.53	0.21
1-C_4H_8	0.51	0.48	0.31	0.25
trans-2-C_4H_8	0.23	0.21	0.17	0.10
cis-2-C_4H_8	0.35	0.28	0.27	0.14
C_2H_6/C_2H_4 ratio	1.81	1.80	1.45	1.60
cis/trans-2-C_4H_{10} ratio	1.52	1.33	1.58	1.40

[a] Relative to the hydrogen balance for H_2 and relative to the ethyl carbon balance for hydrocarbon yields. [b] Ar-flushed prior to thermolysis.

Table VIII. Gaseous Photolysis Products of 5 under Various Conditions

products	% yields[a] under photolysis conditns: solid	H_2O suspensn	CH_3OH soln
H_2	5.60	4.77	0.090
CH_4	0.006	0.008	0.090
C_2H_6	9.83	37.6	52.0
C_2H_4	24.8	28.6	26.0
C_3H_8	0	0	0
C_4H_{10}	trace	1.54	3.72
1-C_4H_8	trace	trace	trace
trans-2-C_4H_8	0	trace	trace
cis-2-C_4H_8	0	trace	trace
C_2H_6/C_2H_4 ratio	0.40	1.31	2.00

[a] Relative to the hydrogen balance for H_2 and relative to the ethyl carbon balance for hydrocarbon yields.

Table IX. Gaseous Products of Anaerobic Hydrolysis of 5 in Different Media

products	% yields[a] under hydrolysis conditns: H_3PO_4 (85%) 20 °C	H_3PO_4 (85%) 95 °C	H_2O 20 °C	H_2O 95 °C	NaOH (50%) 20 °C	NaOH (50%) 95 °C
H_2	0	0	0	0	0	0
CH_4	0.010	0.010	0.002	0.008	0	0.010
C_2H_6	49.7	50.9	0.23	39.1	0.036	97.8
C_2H_4	49.5	49.1	0.23	28.5	0.035	1.66
C_3H_8	0.013	0.013	0	0.007	0	0.049
n-C_4H_{10}	0.033	0.033	0	0.023	0	0.070
1-C_4H_8	0.012	0.014	0	0.010	0	trace

[a] Relative to the ethyl carbon balance. Traces of C_4 hydrocarbons were detected but are not included. All hydrolysis experiments were performed under anaerobic conditions (Ar atmosphere).

Mo–C Bond Hydrolysis. Hydrolysis experiments were performed with samples of 4 mg of **5** in serum-capped Pyrex test tubes protected against light with aluminum foil. At $t = 0$, 85% H_3PO_4, H_2O, or 50% NaOH was injected into the tubes. Hydrocarbon and hydrogen yields were measured by GLPC as described above after 1 h of reaction at 20 and 95 °C, respectively. The results are summarized in Table IX.

Discussion

Synthesis of the Compounds. Reaction of I with stoichiometric amounts of higher n-alkylmagnesium halides was previously shown to yield near 1:1 alkane–alkene mixtures and reduced, presumably Mo(IV)–bpy complexes, instead of the desired di-n-alkyl derivatives. We have since

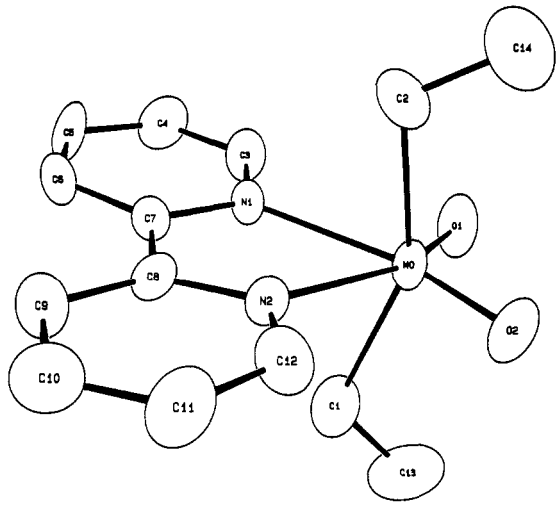

Figure 1. Perspective view of $Mo(O)_2(C_2H_5)_2(bpy)$ with atoms numbered.

found that the Mo(IV) species are realkylated in the presence of excess organomagnesium reagent to yield unstable, saltlike organomolybdenum intermediates from which the neutral dialkyls are released on aerobic hydrolysis (eq 1).

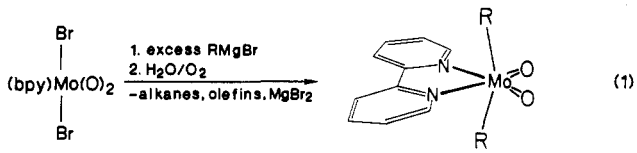

(1)

5, R = C_2H_5
6, R = *n*-C_3H_7
7, R = *i*-C_3H_7
8, R = *n*-C_4H_9
9, R = *i*-C_4H_9
10, R = *c*-C_5H_9
11, R = *c*-C_6H_{11}

Structure. Our knowledge of the structures of the new compounds is based on spectroscopic evidence and a single-crystal x-ray crystallographic analysis of the prototype complex **5**. The structure without the hydrogen positions is shown in Figure 1. No significant differences of bond lengths and bond angles were observed in the $(bpy)Mo(O)_2$ moieties of **5**, **2**, and **3**; see Tables III and IV and ref 4 and 5, and hence discussion of these structural details is not necessary. While the average Mo–C bond distances of 2.20 (2) Å are virtually identical with those in **2** and thus reveal the absence of steric Mo–C bond weakening effects. However, the C–Mo–C angle in **5** of 151.9 (3)° is 2.9° and 6.1° larger than that in **2** and **3**, respectively. Thus far, the only wider C–Mo–C angle [155.5 (8)°] was observed[6] in **6**, where it was attributed to an unusual CT-type interaction of the benzyl phenyl rings with the bpy ligand. While similar interactions are obviously not possible in the dialkyl complexes, indications for interactions of the terminal methyl group hydrogen atoms with the oxygens of the $Mo(O)_2$ moiety have been observed which could be responsible for the widening of the C–Mo–C angle. The methyl groups in **5** are nearly centered above and below the midpoint of the O1/O2 vector. Although the positions of the hydrogen atoms could not be located because of the high thermal motions of C13 and C14, the rather short distances between C13 to O1 and C14 to O2 of 3.2–3.4 Å are suggestive of alkyl—H···O=Mo interactions. These interactions could provide a low-energy pathway for β-elimination reactions in terms of eq 2a, although the C_2H_4 elimination could also occur via intermediate hydridomolybdenum species as indicated in eq 2 b. Depending

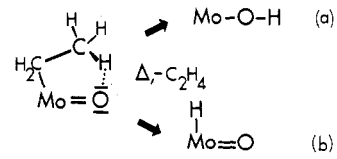

(2)

on the reaction conditions, both types of β-elimination could occur in concurrently with other modes of Mo–C bond cleavage. However, in the following discussion, no specific distinction between the two types of eliminative Mo–C bond cleavage will be made.

Properties and Spectra. All the new higher di-*n*- or dicycloalkyl complexes are thermally significantly less stable than the previously known compounds of this type. The thermal stabilities appear to be primarily dependent on the number of hydrogen atoms in a β-position relative to Mo and the size of R, which, together with electronic factors, determine Mo–C bond strengths. Mo–C bond energy has previously been correlated with energy of the first absorption in the UV–vis spectra of the complexes, as this band appears to be due to a $n-\sigma^*_{Mo-C}$ transition. The decomposition temperatures of complexes **2**–**11** are directly correlated with the energy of this transition with $r = 0.72$ ($P < 0.01$), suggesting that the decomposition temperatures are largely determined by the Mo–C bond strengths. The fact that in complexes **2** and **3** Mo–C bond rupture occurs homolytically rather than by way of β-elimination is evidently responsible for their significantly higher thermal stability as compared to the complexes with β-hydrogens. Steric weakening of the Mo–C bond in **3**, furthermore, is obviously causing its lower thermal stability compared to **2**. Since the Mo–C bond length in **5** is not significantly greater than in **2**, its lower stability must be due to the availability of the β-elimination pathway for Mo–C bond cleavage. This is also obviously true for the secondary and cycloalkyl complexes **7** and **9**–**11**, although in these cases steric effects undoubtedly cause additional Mo–C bond labilization.

Thermolysis. Mixtures of unrearranged alkanes and 1-olefins in the ratios between 1:1 and 2:1 are the main gaseous hydrocarbon thermolysis products of complexes **5**–**9**, while **10** and **11** yield the corresponding cycloalkanes and cycloalkenes in similar proportions. In addition, traces of hydrogen and of other hydrocarbon products are formed, as will be exemplified in greater detail only for the thermolysis of **5**.

On heating of **5** to 300 °C, the formation of C_2H_6 and C_2H_4 is essentially complete in 30 s (see Figure 2). On heating in an argon atmosphere, these two hydrocarbons account for 83.6% of the total ethyl carbon balance (see Table VII). Mo–C bond cleavage by β-elimination appears to be the major mechanism of C_2H_4 formation. This produces a fragment from which C_2H_6 is generated by a reductive Mo–C bond cleavage, as indicated in eq 3.

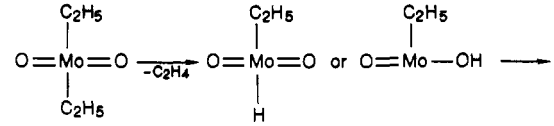

(3)

However, the yields of C_2H_4 in the gas-phase are always somewhat lower than expected according to eq 2. The losses are attributed to polymerization and other side reactions which account for 15–20% of the total ethyl hydrocarbon balance. In addition of C_2H_6 and C_2H_4, traces of CH_4, C_3H_8, *n*-C_4H_{10}, 1-C_4H_8, and H_2 are generated. These products are formed much more slowly than the C_2 hydrocarbons and thus evidently by different mechanisms.

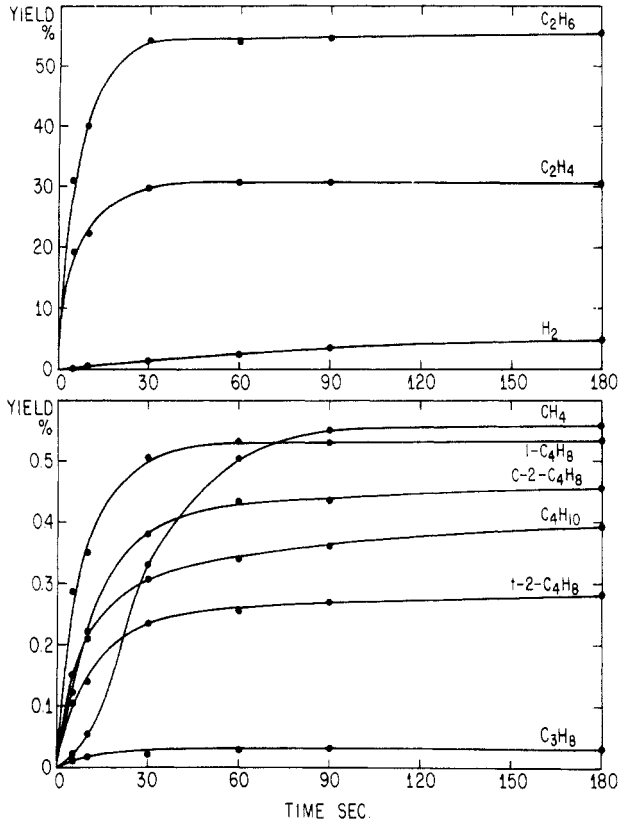

Figure 2. Time course of hydrocarbon and H_2 production on thermolysis of **5** in argon at 300 °C.

Some Mo–C bonds are apparently cleaved homolytically, giving rise to C_2H_5 radicals which dimerize to n-C_4H_{10}. The formation of 1-C_4H_8 suggests that C_2H_4 inserts into thermally excited Mo–C_2H_5 bonds, giving rise to Mo–C_4H_9 residues whose decomposition could yield 1-C_4H_8. The production of *cis*- and *trans*-2-C_4H_8 could be formulated by way of intermediate carbene species as shown in eq 4.

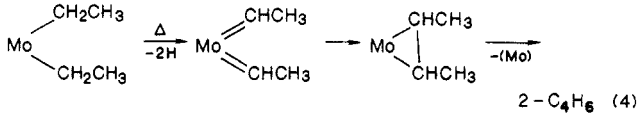

The presence of C_3H_8 and of CH_4 among the thermolysis products suggests that cracking as well as metathesis reactions occur during thermolysis. In silicone oil, a high-boiling solvent with abstractable aliphatic hydrogen, thermolysis of **5** resulted in higher yields of C_2 hydrocarbons and depression of all other hydrocarbon byproducts (see Table VII), as would be expected for reactions involving free organic radicals. The total hydrocarbon balance under these conditions of thermolysis approaches 91% as compared to 86% on thermolysis of solid **5**. The unaccounted for ethyl group carbons are apparently converted to nonvolatile products by process(es) which are probably also associated with the slow evolution of H_2 (see Figure 2).

Hydrogen in the thermolysis gas phase has only a slight effect on hydrocarbon product distribution. Evidently, H_2 is not activated and no efficient mechanism of formation of a reactive hydridomolybdenum species is available under these reaction conditions. On thermolysis of **5** in the presence of O_2, significantly lower yields of C_2H_6 and of H_2 and increased yields of C_2H_4 and of n-C_4H_{10} are observed, suggesting that intermediate radical species are oxidized; however, in complexes of this type, no efficient mechanism of hydrocarbon oxidation is available. We believe that these observations will be helpful in our studies aiming at understanding of the reactivity of molybdena–alumina catalysts with hydrocarbon substrates.

Mo–C Bond Photolysis. On photolysis of solid **5** under argon, C_2H_4 is the main hydrocarbon product; some C_2H_6 and H_2 are also formed (Table VIII). Similar absolute yields of C_2H_4 are observed on photolysis of **5** in methanolic solution; however, C_2H_6 becomes the main product, while H_2 formation is almost completely suppressed. These results suggest that a hydridoethylmolybdenum species is the primary product of photolysis of **5** which decomposes with H_2 evolution in the solid state. In CH_3OH, however, it apparently dissociates, giving rise to an anionic species which decomposes to yield C_2H_6 by reductive Mo–C bond cleavage (see eq 5). In CH_3OH,

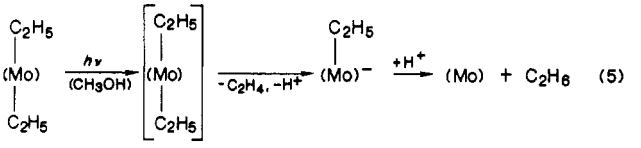

photohomolysis reactions of Mo–C bonds occur as well, as evidenced by the presence of n-C_4H_{10} in the gas phase. On photolysis of aqueous suspensions of **5** the product distribution is intermediate between that in CH_3OH and in the solid state (Table VIII).

Mo–C Bond Solvolysis. Complex **5** reacts with water very slowly at 23 °C, as evidenced by the formation of traces of an equimolar mixture of C_2H_4 and C_2H_6. At 95 °C, however, the decomposition is 70% complete after 1 h, giving rise to C_2H_4 and C_2H_6 in the molar ratio of 0.73. In addition, traces of CH_4, C_3H_8 and C_4 hydrocarbons are formed due to simultaneous Mo–C bond thermolysis. As with the previously described complexes of this series, decomposition of **5** by 50% NaOH is slow at room temperature; on prolonged heating to 95 °C, decomposition to C_2H_6, MoO_4^{2-}, and bipyridyl is quantitative (see Table IX). The behavior of **5** thus is qualitatively similar to that of complexes **2** and **3** and demonstrates the carbanionic character of the Mo-bound C_2H_5 groups.

In the decomposition of **5** in H_3PO_4, on the other hand, one Mo–C bond is cleaved by way of β-elimination and the second reductively, as evidenced by the observed C_2H_4/C_2H_6 ratio. In this case, the reaction is presumably initiated by a protonation of one of the Mo=O residues.

Acknowledgment. This work was supported by Grant CHE 84-14567 of the National Science Foundation.

Registry No. **1**, 25411-14-7; **5**, 104876-01-9; **5**·$^1/_5CH_2Cl_2$, 104876-08-6; **6**, 104876-02-0; **7**, 104876-03-1; **8**, 104876-04-2; **9**, 104876-05-3; **10**, 104876-06-4; **11**, 104876-07-5; C_2H_5Br, 74-96-4; n-C_3H_7Br, 106-94-5; i-C_3H_7Br, 75-26-3; n-C_4H_9Br, 109-65-9; i-C_4H_9Br, 78-77-3; c-C_5H_9Br, 137-43-9; c-$C_6H_{11}Br$, 108-85-0.

Supplementary Material Available: A table of anisotropic thermal parameters (1 page); a listing of observed and calculated structure factors (9 pages). Ordering information is given on any current masthead page.